# Inter-comparison of surface meltwater routing models for the Greenland Ice Sheet and influence on subglacial effective pressures

Kang Yang[1,2], Aleah Sommers[3], Lauren C. Andrews[4], Laurence C. Smith[5,6,7], Xin Lu[1,2], Xavier Fettweis[8], Manchun Li[1,2]

5  [1]School of Geography and Ocean Science, Nanjing University, Nanjing, China
[2]Jiangsu Provincial Key Laboratory of Geographic Information Science and Technology, Nanjing, China
[3]Climate and Global Dynamics Laboratory, National Center for Atmospheric Research, Boulder, CO, USA
[4]Global Modeling and Assimilation Office, NASA Goddard Space Flight Center, Greenbelt, MD, USA
[5]Institute at Brown for Environment and Society, Providence, RI, USA
10  [6]Department of Earth, Environmental & Planetary Sciences, Brown University, Providence, RI, USA
[7]Department of Geography, University of California, Los Angeles, Los Angeles, CA, USA
[8]Department of Geography, University of Liège, Liège, Belgium

*Correspondence to*: Kang Yang (kangyang@nju.edu.cn)

**Abstract.** Each summer, large volumes of surface meltwater flow over the Greenland Ice Sheet (GrIS) surface and drain

15  through moulins to the ice sheet bed, impacting subglacial hydrology and ice flow dynamics. Runoff modulations, or routing delays due to ice surface conditions, thus propagate to englacial and subglacial hydrologic systems, requiring accurate assessment to correctly estimate subglacial effective pressures and short-term lags between climatological melt production and ice velocity. This study compares hourly supraglacial moulin discharge simulations from three surface meltwater routing models, the Synthetic Unit Hydrograph (SUH), Surface Routing and Lake Filling (SRLF), and Rescaled Width Function

20  (RWF), for four internally drained catchments (IDCs) located on the southwestern GrIS surface. Using surface runoff from the MAR regional climate model (RCM), simulated values of surface meltwater transport velocity, flow length, total transport time, unit hydrograph, peak moulin discharge, and time to peak are compared among the three routing models. For each IDC, modeled moulin hydrographs are also input to the SHAKTI subglacial hydrologic model to simulate corresponding subglacial effective pressure variations in the vicinity of a single moulin. Two routing models requiring use of

25  a digital elevation model (SRLF, RWF) are assessed for the impact of DEM spatial resolution on simulated moulin hydrographs. Results indicate SUH, SRLF, and RWF perform differently in simulating moulin peak discharge and time to peak, with RWF simulating slower, smaller peak moulin discharges than SUH or SRLF. SRLF routing is sensitive to DEM spatial resolution, whereas RWF is not. Seasonal evolution of supraglacial stream/river networks is readily accommodated by RWF but not SUH or SRLF. In general, all three models are superior to simply using RCM output without routing, but

30  significant differences among them are found. This variability among surface meltwater routing models is reflected in SHAKTI subglacial hydrology simulations, yielding differing diurnal effective pressure fluctuations.

## 1 Introduction

Large volumes of meltwater are routed through supraglacial stream/river networks across the ablation zone of the Greenland ice surface each summer (Smith et al., 2015). In temperate areas of the ice sheet, most of this surface meltwater can be injected to the bed via moulins (Catania et al., 2008; Lampkin and VanderBerg, 2014; Smith et al., 2015; Yang and Smith, 2016; Koziol and Arnold, 2018), where it can modulate ice flow (Bartholomew et al., 2011; Palmer et al., 2011; Banwell et al., 2013; Hewitt, 2013; Andrews et al., 2014; de Fleurian et al., 2016). However, the role of the supraglacial system in controlling subglacial hydrology remains poorly studied to date (Flowers, 2018). In particular, there are limited constraints on surface meltwater routing efficiencies (Smith et al., 2017), resulting in large uncertainties in hydrodynamic coupling with ice motion.

In most studies that investigate surface-to-bed meltwater connections and the behaviour of the subglacial hydrologic system, surface meltwater routing is either simplified or simply ignored, i.e., moulin hydrographs are estimated directly from output of regional climate models (RCMs) (Flowers, 2018). In the latter instances, RCM instantaneous runoff is simply summed over a given drainage catchment to estimate supraglacial moulin discharge, to drive models of subglacial hydrologic system evolution and/or ice flow dynamics (Bartholomew et al., 2011; Bartholomew et al., 2012). This simplification may be appropriate for small drainage catchment or for long-term studies; however, surface meltwater routing has been found to substantially modify ice surface runoff (Banwell et al., 2012; Banwell et al., 2013; Arnold et al., 2014), thus altering the magnitude and timing of peak moulin discharge (Smith et al., 2017; Yang et al., 2018). As such, supraglacial routing has strong potential to affect subglacial hydrologic system evolution and hydrodynamics, especially for large catchments and short (i.e., diurnal) time scales.

Surface meltwater routing may be characterized by meltwater transport velocity ($v$), flow length ($L$), and transport time ($t$). Meltwater transport velocity and flow length can be estimated from ice surface topography (Arnold et al., 1998), with the distribution of transport times representing the hydrologic response of a particular supraglacial catchment to surface melt (Yang et al., 2018). Alternately, empirical unit hydrograph (UH) methods can be used to estimate the hydrologic response based on catchment shape and area alone, enabling derivation of moulin hydrographs through convolution of input RCM surface runoff with remotely-sensed UH parameters (Smith et al., 2017).

The DEM-based Surface Routing and Lake Filling (SRLF) model was developed to route supraglacial meltwater on ice surfaces (Arnold et al., 1998; Banwell et al., 2012). SRLF assumes all meltwater is transported downslope, with Manning's open-channel flow equation used to calculate spatially variable meltwater transport velocities for every bare-ice DEM pixel.

More recently, the Snyder Synthetic Unit Hydrograph (SUH) (Snyder, 1938) was adapted for use on ice sheets to estimate moulin hydrographs without the need for a DEM (Smith et al., 2017). To do this, two key SUH coefficients were calibrated using a field-measured moulin hydrograph, and a Gamma function was then used to build individual SUHs for hundreds of remotely-sensed IDCs (Smith et al., 2017). Because the Snyder SUH is a simple lumped model that does not rely on DEMs, it provides a straightforward (if static) approach to route surface meltwater to moulins.

Most recently, Yang et al. (2018) utilized Rescaled Width Function (RWF) (D'Odorico and Rigon, 2003) to further partition the bare ice surface into either interfluve (i.e., hillslope) or open-channel zones using high-resolution satellite imagery discern the two. Catchment-averaged meltwater transport velocities for each zone were then calibrated using a field-measured moulin hydrograph (Smith et al., 2017), with slow interfluve flow ($\sim10^{-3}$-$10^{-4}$ m/s) and fast open-channel flow ($\sim10^{-1}$ m/s) combined to simulate the downstream moulin hydrograph.

These three surface meltwater routing approaches have different assumptions and data requirements. SUH is the simplest model; it only requires catchment shape and area to estimate surface meltwater transport time (Smith et al., 2017). In contrast, the generally ad hoc partitioning of slow and fast flow can substantially impact the performance of SRLF and RWF without careful calibration. Moreover, SRLF and RWF rely on surface DEMs to calculate meltwater flow paths (Yang et al., 2018) and SRLF also relies on DEMs to calculate meltwater routing velocities (Arnold et al., 1998). Characteristics such as slope, flow direction, flow length, drainage area, and drainage networks are readily extracted from DEMs but are scale-dependent (Montgomery and Foufoula-Georgiou, 1993), signifying that DEM spatial resolutions influence their computation (Zhang and Montgomery, 1994; Hancock et al., 2006). This DEM resolution dependence can now be tested with the advance of high-resolution DEM datasets (e.g., 2 m ArcticDEM) of the GrIS surface (Noh and Howat, 2015, 2017, 2018).

To assess these differences among different routing models, this study simulates surface meltwater through four moderate-size IDCs using the SUH, SRLF, and RWF models. Their capabilities in simulations of meltwater transport velocity, flow length, transport time, UH, peak moulin discharge, and time to peak are compared, and the impact of DEM spatial resolution on SRLF and RWF is examined. For all of these models, the consequent effect of using them to drive subglacial effective pressure variations is investigated for the simple illustrative case of meltwater input to the bed via a single moulin, using the Subglacial Hydrology and Kinetic, Transient Interactions (SHAKTI) subglacial hydrologic model (Sommers et al., 2018). We conclude with a general discussion of surface meltwater routing on the Greenland ice surface and include some recommendations for best practices and future research.

## 2 Study area and data sources

Four moderate-size supraglacial IDCs were selected to explore the impact of SUH, SRLF, and RWF meltwater routing models on moulin discharge and subglacial effective pressure (Figure 1, Table 1). They are distributed at approximately 200 m elevation intervals in order to span the elevational range of most well-developed IDCs found on the southwestern GrIS (Yang and Smith, 2016). Their areas range from 53.0 km$^2$ to 66.9 km$^2$; surface elevations vary from 1086 m to 1672 m and ice thicknesses from 854 m to 1432 m (Table 1).

The high-resolution (2 m) ArcticDEM is the primary data source for our study of surface meltwater routing in the four supraglacial IDCs. ArcticDEM products are created from high-resolution (0.5 m) WorldView-1/2/3 stereo images by Polar Geospatial Center (PGC) and provide an unprecedented opportunity to investigate ice surface landscape and hydrologic

processes (Noh and Howat, 2015, 2017, 2018). MAR (Modèle Atmosphérique Régionale) 3.6, a regional coupled atmosphere-land climate model with 20 km native horizontal resolution (Fettweis et al., 2013), provides hourly surface runoff simulations.

## 3 Methods

### 3.1 RCM runoff simulations

Hourly simulations of surface runoff during July 2015 were obtained from MAR 3.6. Supraglacial IDC boundaries were derived from ArcticDEM following the method of Karlstrom and Yang (2016). Catchment-averaged hourly runoff [mm/h] was obtained by clipping MAR grid pixels with the supraglacial IDC boundaries and summing their corresponding runoff values (Smith et al., 2017). Absent any routing, the resulting area-integrated runoff is termed RCM instantaneous runoff.

### 3.2 Snyder Synthetic Unit Hydrograph (SUH)

The Unit Hydrograph (UH) provides a transfer function between surface runoff and moulin discharge $Q$ (i.e., direct hydrograph). Snyder Synthetic Unit Hydrograph (SUH) (Snyder, 1938) assumes catchment morphometry controls the shape of UH and utilizes two coefficients, $C_p$ and $C_t$, to determine peak discharge ($h_p$) and time-to-peak in ($t_p$) of SUH (Singh et al., 2014). Smith et al. (2017) used a field-measured moulin hydrograph to calibrate $C_p$ and $C_t$ and demonstrated coefficient transferability using two other independently field-measured moulin hydrographs (McGrath et al., 2011; Chandler et al., 2013). Following Smith et al. (2017), we use $C_p = 0.72$ and $C_t = 1.61$ to determine $h_p$ and $t_p$ of SUHs and employ a gamma distribution to determine the catchment-specific SUH for each IDC.

### 3.3 Surface Routing and Lake Filling (SRLF)

SRLF is traditionally used to fill supraglacial lakes at the catchment outlet (Banwell et al., 2012). Here we use the model to route surface meltwater downslope to a moulin and subsequently to the ice sheet bed. SRLF assumes universal presence of supraglacial open-channel flow everywhere on bare ice surface, by applying Manning's open-channel flow equation (Manning, 1891) to calculate channelized meltwater velocity $v$ for every pixel along a DEM-derived flow path:

$$v = R_H^{2/3} S^{1/2} / n \quad (1)$$

where $R_H$ is the hydraulic radius of the supraglacial meltwater channel, $S$ is water surface slope calculated from DEM, and $n$ is the Manning roughness coefficient (Arnold et al., 1998). Following Arnold et al. (1998), we set $R_H = 0.035$ m and $n = 0.05$. $S$ was calculated per pixel using ArcticDEM. The shortest meltwater flow length ($L$) was determined from ArcticDEM using the D8 flow routing algorithm following Karlstrom and Yang (2016). Meltwater transport time ($t$) for each DEM pixel was then determined as $t = L/v$. To compare with SUH and RWF, a one-hour UH was calculated by hourly binning the transport time raster (Yang et al., 2018), with the resultant UH termed SRLF-UH.

### 3.4 Rescaled Width Function (RWF)

The rescaled width function (RWF) routing model partitions surface meltwater transport pathways into hillslope and open-channel distances ($L_h$ and $L_c$), to determine two catchment-averaged meltwater velocities ($v_h$ and $v_c$) to represent routing efficiency over these regions (D'Odorico and Rigon, 2003). Then, the transport time for each pixel in a catchment may be calculated as:

$$t = t_h + t_c = \frac{L_h}{v_h} + \frac{L_c}{v_c} \quad (2)$$

Similar to SRLF, the shortest meltwater flow path for interfluve (hillslope) and channel transport distances is determined using a DEM (Karlstrom and Yang, 2016), with the relative coverage determined by the extent of supraglacial streams and rivers (Yang et al., 2018). By applying the constant $v_h$ to interfluve pixels and $v_c$ to open channel pixels, the meltwater transport time from every catchment pixel to the moulin can be determined and a consequent catchment UH generated, hereafter referred to as RWF-UH. Using the in situ moulin hydrograph of Smith et al. (2017), Yang et al. (2018) determined the velocity combination of $v_h = 0.0006$ m/s and $v_c = 0.4$ m/s to be the optimal match to field observations. In this study, the velocity combination is assumed to be transferable and used to create RWF-UHs for the four IDCs.

It is impossible to determine which of the three models compared here is "best" (i.e., best able to reproduce a real-world moulin hydrograph) due to the lack of a second, continuously acquired moulin discharge dataset. Owing to this limitation, the goal of this research is to assess differences among the three meltwater routing models, rather than revealing which model most realistically simulates surface meltwater routing on the ice surface. By using the outputs from all three as meltwater inputs to drive the SHAKTI subglacial model, we characterize the impact of their differences on subglacial effective pressure, and, more generally, the importance of routing supraglacial runoff on subglacial conditions.

### 3.5 Controls of DEM resolution on surface meltwater routing

To estimate the control of DEM spatial resolution on ice surface meltwater routing, 2 m resolution ArcticDEM data were resampled to 5 m, 10 m, 30 m, and 90 m resolutions, similar to Zhang and Montgomery (1994), and the corresponding meltwater flow paths, velocities, transport time, UHs, and moulin hydrographs from SRLF and RWF subsequently calculated. For SRLF, all five resampled DEMs were used. For RWF, only 2 m, 5 m, and 10 m resolutions were used to prevent DEM resolution from exceeding the typical interfluve transport distance, ~10 m for southwestern GrIS (Yang et al., 2018). Otherwise, hillslope transport distance would be overestimated and the resultant hydrograph would be inappropriate (Zhang and Montgomery, 1994; Hancock et al., 2006).

### 3.6 Temporal evolution of surface meltwater routing

The spatial pattern of supraglacial stream/river networks is known to vary significantly during a melt season (Lampkin and VanderBerg, 2014). This affects the hydrologic response (and UH) of a supraglacial IDC as transport distances change (Montgomery and Foufoula-Georgiou, 1993). RWF can mimic this effect by varying the partitioning of hillslope versus

open-channel zones (Yang et al., 2018). SUH and SRLF, in contrast, assume a stable response because in practice they typically assume a fixed catchment extent or a static DEM, respectively.

Capturing the rapid seasonal evolution of supraglacial stream/river networks is challenging (Lampkin and VanderBerg, 2014; Yang et al., 2017) and remains largely undone (Flowers, 2018), but a positive relationship exists between surface melt and supraglacial drainage density (Yang et al., 2017; Yang et al., 2019). As a simplified simulation, this study uses a series of cumulative contributing area ($A_c$) values ($A_c$ = 100 m$^2$, 250 m$^2$, 500 m$^2$, 1000 m$^2$, 2500 m$^2$, 5000 m$^2$), which define the surface area needed to initiate open channel flow, to simulate the hypothetical seasonal evolution of supraglacial stream/river networks by evolving the partitioning of interfluve vs. open channels and resultant surface meltwater routing simulations (Yang et al., 2018). Smaller values of $A_c$ signify periods of intense surface melt and actively flowing, well-developed supraglacial stream/river networks (Smith et al., 2017), whereas larger values signify poorly developed network characteristics of the late melt season (Yang et al., 2018). A total of six 5-day RWF-UHs were created for each $A_c$ value, broadly consistent with a decreasing RCM runoff trend during July 2015.

## 3.7 Subglacial hydrology modeling

A variety of numerical models have been formulated to simulate different aspects of the subglacial drainage system and derive subglacial effective pressure (Flowers, 2015; de Fleurian et al., 2018). To examine the variations in modeled effective pressure resulting from the different surface meltwater routing models considered in this study, we treat their respective outputs as direct meltwater inputs to the bed via a single moulin, and simulate subsequent evolution of the subglacial drainage system using the SHAKTI model (Sommers et al., 2018).

SHAKTI is built into the Ice Sheet System Model framework (Larour et al., 2012). Using finite elements, it applies a single set of equations over the entire model domain, with a subglacial water flux formulation allowing for local development of both turbulent and laminar flow regimes, as well as regimes corresponding to the broad transition between laminar and turbulent. SHAKTI calculates transient effective pressure, hydraulic head, subglacial gap height, subglacial water flux, and "degree of channelization" (defined as the ratio of the rate of opening by melt to the rate of opening by sliding over bumps in the bed). Subglacial effective pressure and geometry evolve naturally to produce continuous configurations ranging from sheet-like to channelized drainage. A thorough description of the SHAKTI model equations, methods, and features can be found in Sommers et al. (2018).

To examine the influence of different surface meltwater routing models on subglacial hydrology in an isolated setting, we apply meltwater input at a single moulin at the center of a 1 km square domain. The domain is discretized with an unstructured triangular mesh consisting of 614 elements and a typical element edge length of 50 m (Figure 2). Outflow is to the left edge of the square domain, with a Dirichlet boundary condition set to atmospheric pressure, and zero-flux pressure boundaries on the other three sides. For each IDC, the surface and bed slopes are fixed at 0.02 and their mean ice thickness used (Table 1). The SHAKTI model was run as a stand-alone model for these simulations, with a uniform, constant ice sliding velocity of 10$^{-6}$ m s$^{-1}$ (approximately 31 m a$^{-1}$). Each transient simulation was initialized with the subglacial effective

pressure equal to 50 % of the ice overburden pressure. Constants and parameter values used in the simulations are summarized in Table 2.

## 4 Results

### 4.1 Simulations of supraglacial moulin discharge

5      Inclusion of surface meltwater routing clearly modifies the timing of peak moulin discharge relative to RCM runoff obtained from MAR climate model, with each of the three routing models performing somewhat differently. When RCM instantaneous runoff alone is used to simulate moulin discharge (i.e., no routing), moulin discharges peak between 13:00-15:00 local time for all the four study IDCs. Inclusion of routing processes, however, introduces considerable lags between the timing of peak runoff generation in each IDC and its arrival at the moulins, ranging from 17:00 to 23:00 local time (Table 1, Figures 3 and S1-S3). SUH-routed hydrographs simulate peak moulin discharge between approximately 19:00 and 21:00, a delay of 6 hours compared to the RCM instantaneous peak discharge, while RWF-routed delay varies from 7 hours to 10 hours and SRLF-routed delays varies from 3 hours to 10 hours (Table 1). In general, these delays are much longer than ~2 hours measured for small IDCs near ice margins (Shepherd et al., 2009; McGrath et al., 2011; Bartholomew et al., 2012) but are comparable to ~5-7 hours measured for a ~60 km$^2$ IDC, confirming the control of catchment size on surface meltwater routing delays (Smith et al., 2017).

Surface meltwater routing also controls peak moulin discharge magnitude and diurnal discharge range. RWF-UHs are smoother than SUHs and 2 m SRLF-UHs (Figures 3a, 3d, and 3g). For IDC1, the peak RWF-UH is ~0.10 (Figure 3g), indicating that ~10 % surface meltwater is routed to the moulin during the peak runoff hour (Singh et al., 2014), while the peak values are ~0.13 for SUH  (Figure 3a) and ~0.15 for 2 m SRLF-UH (Figure 3d). With smoother UHs yielding smaller peak moulin discharge magnitudes and diurnal discharge ranges, inclusion of surface meltwater routing introduces smaller peak moulin discharge relative to the RCM instantaneous peak discharge (Figures 3b, 3e, and 3h). For IDC1, the peak moulin discharges simulated by the three routing models are >25 % higher than the RCM instantaneous peak moulin discharge, while the diurnal discharge ranges are >27 % higher. Among the three routing models, RWF introduces slightly smoother moulin hydrographs than SUH and 2 m SRLF (Figures 3b, 3e, and 3h), yielding small differences in peak moulin discharge (<7%) and diurnal discharge range (<12%). This finding suggests that all three models are more representative of the observed processes than using RCM instantaneous runoff without routing, but that each model collects and distributes surface meltwater with different efficiency.

### 4.2 Long-term evolution of moulin discharge simulations

Long-term evolution of supraglacial stream/river networks is found to substantially alter surface meltwater routing processes and to yield highly dynamic UHs and moulin discharges (Figures 3k, 3i, and 4). This result is consistent with

Montgomery and Foufoula-Georgiou (1993), which found that river network extent controls the response of catchments to precipitation (melt in our case). To illustrate the strong potentially dynamism of network extent on bare ice, Figure 5 presents dynamic supraglacial stream/river networks of IDC1 under different $A_c$ thresholds, with drainage density varying from 19.3 $m^{-1}$ to 0.8 $m^{-1}$. Such strong, seasonal variation in supraglacial stream/river network extent is well-supported by previous high-resolution remote sensing studies, which report similar expansion and contraction of actively flowing supraglacial stream/river networks during the melt season (Smith et al., 2015; Smith et al., 2017; Yang et al., 2018).

Well-developed supraglacial stream/river networks (e.g., simulated using $A_c = 100$ $m^2$) route surface meltwater efficiently (Smith et al., 2015), yielding high UH and moulin discharge peaks, whereas relatively poorly-developed supraglacial stream/river networks indicate relatively slow routing of meltwater in expanding hillslope zones (Yang et al., 2018), yielding smaller and delayed UH and moulin discharge peaks (Figures 3j and 3k). Our simple modeling experiment (by increasing $A_c$ thresholds every 5 days for the month of July 2015) suggests a gradual dampening of diurnal variations until, by the end of the month, such variations are ~50 % smaller than the same routing method using a smaller $A_c$ value (Figure 3k).

## 4.3 Effects of DEM spatial resolution on surface meltwater routing

RWF routing is largely unaffected by DEM spatial resolution, but SRLF routing is significantly affected. Resampling 2 m ArcticDEM data to 5 m and 10 m yields similar RWF-UHs and moulin discharges (Figures 3g and 3h), but progressively smoother versions using SRLF-UHs (Figures 3d and 3e). At 90 m resolution, SRLF-UH shapes exhibit diminished and delayed peaks (Figure 3d). For IDC1, for example, use of a 90 m DEM yields a ~0.10 UH peak at hour 9 and a ~0.04 UH peak at hour 17, whereas 2 m DEM yield a ~0.15 UH peak at hour 5 with all meltwater evacuated within 15 hours.

SRLF applied on higher-resolution DEMs yields larger peak moulin discharges and diurnal discharge signals (Figure 3e). For IDC1, SRLF-routed peak moulin discharge derived from 2 m DEM is 52.4 % larger than that from 90 m DEM, while the corresponding value for SRLF-routed diurnal discharge range is 179.0 %. This finding indicates that SLRF performance is strongly controlled by DEM spatial resolution, with coarser resolutions resulting increased damping of simulated moulin hydrographs.

## 4.4 Subglacial effective pressure

When applied to provide meltwater input to the bed via a single moulin, the SRLF, SUH, and RWF meltwater routing models all introduce diurnal and long-term fluctuations in subglacial effective pressure, shown for IDC1 in Figure 3. Interestingly, the mean effective pressure over the 31-day period is relatively consistent between models, varying by < 4% (ranging from 4.69 MPa in the SUH model to 4.87 MPa in the SLRF model with 90 m resolution) for IDC1. The amplitude of the fluctuations around the mean, however, differs substantially between different routing models and DEM resolutions (Figures 3 and S1-S3).

The relative magnitudes of diurnal signals seen in the meltwater inputs are reflected in the subglacial response. The effective pressure amplitude scales relative to the meltwater input amplitude, with the largest amplitude produced by the RCM instantaneous runoff inputs (Figures 3c, 3f, 3i, and 3l). While all surface meltwater routing models dampen these amplitudes as compared to RCM instantaneous runoff, the models that produce relatively high-amplitude moulin inputs

5    correspond to high-amplitude effective pressure variations, notably in the 2 m SLRF method which frequently yields zero effective pressure and a diurnal amplitude of ~ 4.5 MPa (Figure 3f). With 90 m DEM resolution, the diurnal amplitude decreases to < 1 MPa. In the dynamic RWF method, the dampening effect displayed in the moulin inputs carries over into the resulting effective pressure cycles (Figure 3l).

In all cases a clear preferential pathway develops from the moulin location at the center to the outflow at the left edge of

10    the domain. This efficient channelized drainage pathway evolves and fluctuates with the inputs through time and is characterized by higher gap height and effective pressure (i.e. lower hydraulic head and water pressure) than the surrounding bed in the y direction (Figure 6, Supplementary Animation).

For all surface meltwater routing models, the daily minimum moulin input is followed after a lag of a few hours by the minimum effective pressure (which corresponds to the maximum water pressure, as the subglacial system shuts down due to

15    ice creep in the absence of high meltwater input required to maintain a larger gap height). An example of this timing is readily seen in Figure 7, which presents moulin input using the SUH method overlaid with effective pressure in IDC1.

In general, we find that while the moulin inputs generated by the different surface routing models produce diurnal variations of different magnitude in effective pressure, the overall channelization behavior and mean effective pressure over the 31-day simulations are relatively consistent between models. These results suggest that in a fully coupled ice

20    dynamics/subglacial hydrology model, different routing methods may not produce significantly different cumulative effects in effective pressure for simulation time scales greater than daily.

## 5 Discussion

### 5.1 Implications of surface meltwater routing method inter-comparison

This study conducted an inter-comparison of three surface meltwater routing models (SUH, SRLF, and RWF). Due to

25    the lack of field-measured moulin hydrographs, it is difficult to determine which meltwater routing model performs most realistically in a wide area during a long time period. However, our simulations of moulin discharges (Figures 3, and S1-S3) can provide some insightful information to qualitatively evaluate the performance of certain routing methods. First, inclusion of surface meltwater routing introduces lower peak moulin discharges and delayed time to peak relative to the RCM instantaneous runoff. Second, for IDCs with similar areas and elevations as those examined here, simulated peak moulin

30    discharge consistently occurs between 19:30 and 22:00 (Chandler et al., 2013; Smith et al., 2017). The timing of peak discharge suggests that several routing scenarios are unlikely to be realistic, including any technique that uses RCM alone as

it qualitatively underestimates peak discharge time, and SRLF using high (2 m) and low resolution (30 & 90 m), due to both underestimating and overestimating peak discharge time, respectively.

Additionally, we can use observations of channelized subglacial pressure to strengthen our qualitative comparison. While exact field measurements are not available for direct comparison to our modeled effective pressures, limited field observations indicate that hydraulic head within subglacial channels varies diurnally by at least 40 m and up to 150 m in regions with slightly thinner ice (Cowton et al., 2013; Meierbachtol et al., 2013; Andrews et al., 2014). Furthermore, these reported pressure variations in channelized regions do not fall below ~0.4 of overburden. Our model results for the single-moulin tests, while somewhat dependent on chosen parameterizations, suggest that both RCM only and 2m SRLF do not apply enough delay to ice surface meltwater routing, resulting in modeled effective pressure variations of up to 4.5 MPa in IDC1 (corresponding to ~600 m variation in head; Figure 3f). Combined, these observations suggest that simultaneous RCM runoff is unlikely to provide physically realistic ice surface runoff and the resolution of SRLF needs to be carefully chosen to generate realistic diurnal meltwater inputs to the subglacial drainage system.

## 5.2 Impact of DEM resolution on supraglacial meltwater routing

RWF routing is not affected by DEM spatial resolution, whereas SRLF routing is (Table 1 and Figure 3). The 5 m SRLF-UHs and resultant moulin discharges best match with RWF and SUH simulations (Figure 3 and 4). This is consistent with the finding that "the most appropriate DEM grid size for topographically driven hydrologic models is somewhat finer than the hillslope scale identifiable in the field" (Zhang and Montgomery, 1994). This behavior occurs because a coarser-resolution DEM represents ice surface topography more smoothly and yields lower ice surface slopes, similar to terrestrial topography (Zhang and Montgomery, 1994); lower topographical slopes yield smaller velocities via Manning's open-channel equation.

Different meltwater routing velocities control the meltwater transport time because meltwater flow length is only slightly impacted by DEM resolutions. As a result, lower SRLF meltwater routing velocities induce longer meltwater transport time and distribute diurnal surface runoff more smoothly over time (Figures 3d and 3e), whereas stable flow length contributes to RWF's better performances under different DEM resolutions (Figures 3g and 3h).

## 5.3 Influence of seasonal supraglacial drainage evolution on meltwater routing

Seasonal evolution of ice surface drainage pattern can substantially alter surface meltwater routing and moulin discharge characteristics (Figures 3 and 4). Such changes also involve the removal and deposition of the winter snowpack (Nienow et al., 2017) and the development of a weathering crust on base ice (Cooper et al., 2018), both of which can reduce the prevalence of open-channel flow (Yang et al., 2018). While these processes cannot be explicitly represented with the meltwater routing parameterizations described here, time evolving UHs can integrate the impact of seasonal changes in the

relative proportions of porous and open-channel flow (Figure 5). As such, the relative ease of creating dynamic UHs to mimic seasonal evolution of supraglacial stream/river networks is a distinctive advantage of RWF (Figure 3k and 3l).

The development of time varying UHs provides an opportunity to simulate dynamic moulin discharges (Smith et al., 2017; Yang et al., 2018). Such time-varying UHs could be critical in realistically modeling the evolution of the subglacial
5  drainage system and the development of subglacial channels – a limited supraglacial stream/river extent will dampen the diurnal range of meltwater inputs into the subglacial system and maintain a more constant subglacial pressure (e.g. Figure 3k), which in turn results in less variation in ice motion. Furthermore, limiting diurnal variations may result in more rapid growth of subglacial channels early in the melt season (Schoof, 2010; Hewitt, 2013), thus, potentially produce a more realistic transition to primarily channelized drainage (Banwell et al., 2013; Banwell et al., 2016).

10  **5.4 Influence on diurnal subglacial pressure variations**

Our results demonstrate that the routing models and DEM resolution can modulate the diurnal variability of both surface meltwater transport and associated moulin inputs (Figures 3 and 4). Surface meltwater routing alters hourly inputs, with only slight changes to total integrated daily moulin input. However, hourly variations in moulin discharge can influence ice dynamics. Diurnal variations in subglacial pressure, for example, are directly associated with diurnal variations in ice
15  velocity, which have the capacity to induce additional surface-to-bed connections (Carmichael et al., 2015; Hoffman et al., 2018). The diurnal amplitude of moulin discharge also affects the transient evolution of the subglacial drainage system without sustained input to maintain efficient drainage channels, subglacial effective pressure increases, resulting in increased sliding velocities, potentially influencing seasonal ice displacement (Hewitt, 2013; van de Wal et al., 2015). As such, including the diurnal signal of moulin discharge may be important for accurately modeling surface-to-bed meltwater
20  connections (Figure 3 & S1-S3). However, as described in Section 4.4, the mean effective pressure produced in our subglacial hydrology simulations with inputs from the various routing models is relatively consistent between models. Depending on the time scale of interest, diurnal inputs may not be vital to capture the relevant ice dynamics.

Many subglacial hydrology models commonly invoke a numerical term (the "englacial void ratio") to represent englacial storage in order to provide short term storage and release of meltwater that cannot be accommodated rapidly within
25  the subglacial system, in the absence of more realistic representation of supraglacial and englacial storage (Hewitt, 2013; Werder et al., 2013; Hoffman et al., 2016). In SHAKTI, this englacial void ratio is also included as an option (Sommers et al., 2018), but our simulations considered here do not employ this term in the equations. Our results demonstrate that the supraglacial hydrologic system can act as short-term storage for surface-derived meltwater; therefore, application of an appropriate surface meltwater routing scheme may reduce the dependence of some subglacial models on a somewhat
30  arbitrary englacial storage term to produce realistic diurnal effective pressure variations and timing lags (Werder et al., 2013; Hoffman et al., 2016). The assumption of surface inputs being instantaneously delivered to the subglacial system is an

approximation that ignores the largely uncertain complex flow paths through the englacial system from surface to bed, but it is reasonable to assume that variability in surface inputs should influence variability in inputs to the subglacial system.

Supraglacial routing delays can affect the amplitude and timing of subglacial pressure variations (Figure 7). While there is limited evidence that within a fully coupled ice dynamics/subglacial hydrology model that diurnal variations in effective pressure can contribute to changes in ice dynamics (Hewitt, 2013), the evolution of the supraglacial hydrologic system can substantially alter effective pressure on diurnal timescales (e.g. Figure 3i). Subglacial channel development is key to terminating early melt season accelerated sliding (Hoffman and Price, 2014) and subglacial channelization occurs more readily under constant supraglacial meltwater inputs (Schoof, 2010; Poinar et al., 2019). The appropriate choice of a time evolving surface meltwater routing scheme may, in addition to providing the best representation of diurnal effective pressure variations, result in an improved representation of subglacial evolution and improve quantitative representation of seasonal variations in ice flow in coupled models. Our results, however, show that while meltwater inputs with highly variable diurnal amplitudes yield effective pressures with highly variable diurnal amplitudes, the general channelization behavior and mean effective pressure over the 31-day simulations are quite similar across routing methods. Further work is needed to explore the implications of using sub-daily inputs versus time-averaged inputs on long-term subglacial hydrology and ice dynamics in realistic, large domains. The case may be that the peaks and troughs of large-amplitude diurnal input variations effectively even themselves out to yield equivalent results as time-averaged inputs.

**5.5 Future research directions of surface-to-bed meltwater connection**

A challenge remaining unsolved is to map or simulate seasonal evolution of supraglacial stream/river networks. Spatial extent of supraglacial stream/river networks determine partition of hillslope and open-channel zones and thereby controls IDC hydrologic response to surface melt. Moreover, all three routing models described in this study do not explicitly include complex ice surface composition and transformation, including the retreat of seasonal snow cover (Hubbard and Nienow, 1997) and the modification of the ice surface by incoming solar radiation and other processes in the hillslope zone (Karlstrom et al., 2014; Cooper et al., 2018). This may lead to uncertainties in UH and moulin discharge simulations. Recently, weathering crust has been found to be widely distributed on the Greenland ice surface (Cooper et al., 2018), rather than impermeable bare ice layer as previously assumed (Arnold et al., 1998). Therefore, an appropriate parameterization of porous media flow may be important to accurately describe meltwater transport in the hillslope zone of ice surface (Karlstrom et al., 2014; Cooper et al., 2018; Yang et al., 2018). Additionally, the hourly MAR runoff is a cumulative runoff on one hour and may induce a potential delay of one hour in the peaks; therefore, 10-15 minute MAR runoff should be used to better capture runoff delays in future.

Furthermore, the single-moulin simulations in this study should be interpreted as a focused view into how different meltwater routing methods influence subglacial hydrology in the immediate vicinity of moulins through variations in moulin inputs. Simulations using real surface and bed topographies, moulin locations, and the full IDC areas in a fully coupled ice

dynamics/subglacial hydrology model remain for future work, an important next step in understanding the surface-to-bed meltwater influence on regional and large-scale ice dynamics. A more direct comparison of model results with observations will be appropriate for this future work, in which the entire drainage catchments are modeled with realistic topography and moulin distribution in areas where borehole observations are available or relevant quantities may be inferred from radar
5   products (Chu et al., 2016).

## 6 Conclusions

Surface meltwater routing is crucial for understanding the surface-to-bed meltwater connection of the Greenland Ice Sheet but remains poorly studied to date. This study presents a first inter-comparison of three different meltwater routing models and employs a subglacial hydrologic model to explore the impacts of their differences on subglacial effective pressure in the
10  vicinity of moulins. Results show that inclusion of surface meltwater routing introduces significantly small peak moulin discharges and delayed time to peak relative to the RCM instantaneous runoff. Different surface meltwater routing models, as well as different spatial-resolution DEMs and seasonal evolution of the supraglacial stream/river networks, induce variable diurnal moulin discharges and effective pressures, which influence ice sliding velocity. While the different routing models produce different diurnal amplitudes in effective pressure variation, the overall channelization behavior and mean
15  effective pressures are relatively consistent between models. Together, these findings urge caution for better representations of surface meltwater routing and moulin discharge simulations to drive subglacial hydrology and ice dynamics models, as well as highlight the need for further research to investigate the cumulative effects of diurnal inputs to the subglacial drainage system and the relevant impacts on ice dynamics.

20  **Data availability**

The ArcticDEM data are available at the Public HTTP Data Repository of Polar Geospatial Center at the University of Minnesota (https://www.pgc.umn.edu/data/arcticdem/). Hourly MAR (Modèle Atmosphérique Régionale) 3.6 model data can be accessed by contacting Xavier Fettweis (xavier.fettweis@uliege.be).

**Author contributions**

25  KY and AS designed the study. KY and AS performed the data analysis. KY wrote the paper with contributions from all authors.

**Competing interests**

The authors declare that they have no conflict of interest.

## Acknowledgements

Kang Yang acknowledges support from the National Key R&D Program (2018YFC1406101), the National Natural Science Foundation of China (41871327), and the Fundamental Research Funds for the Central Universities (14380070). Laurence C. Smith acknowledges the support of the NASA Cryosphere Program (80NSSC19K0942) managed by Dr. Thorsten Markus.

5    ArcticDEMs are provided by the Polar Geospatial Center at the University of Minnesota under NSF-OPP awards 1043681, 1559691, and 1542736.

# References

Andrews, L.C., Catania, G.A., Hoffman, M.J., Gulley, J.D., Luthi, M.P., Ryser, C., Hawley, R.L., Neumann, T.A., 2014. Direct observations of evolving subglacial drainage beneath the Greenland Ice Sheet. Nature 514, 80-83.

Arnold, N.S., Banwell, A.F., Willis, I.C., 2014. High-resolution modelling of the seasonal evolution of surface water storage on the Greenland Ice Sheet. Cryosph. 8, 1149-1160.

Arnold, N.S., Richards, K., Willis, I., Sharp, M., 1998. Initial results from a distributed, physically based model of glacier hydrology. Hydrolo. Process. 12, 191-219.

Banwell, A.F., Arnold, N.S., Willis, I.C., Tedesco, M., Ahlstrøm, A.P., 2012. Modeling supraglacial water routing and lake filling on the Greenland Ice Sheet. J. Geophys. Res. 117, F04012.

Banwell, A.F., Hewitt, I., Willis, I., Arnold, N., 2016. Moulin density controls drainage development beneath the Greenland Ice Sheet. J. Geophys. Res. Earth Surf. 121, 2248-2269.

Banwell, A.F., Willis, I.C., Arnold, N.S., 2013. Modeling subglacial water routing at Paakitsoq, W Greenland. J. Geophys. Res. Earth Surf. 118, 1282-1295.

Bartholomew, I.D., Nienow, P., Sole, A., Mair, D., Cowton, T., King, M.A., 2012. Short-term variability in Greenland Ice Sheet motion forced by time-varying meltwater drainage: Implications for the relationship between subglacial drainage system behavior and ice velocity. J. Geophys. Res. Earth Surf. 117.

Bartholomew, I.D., Nienow, P., Sole, A., Mair, D., Cowton, T., King, M.A., Palmer, S., 2011. Seasonal variations in Greenland Ice Sheet motion: Inland extent and behaviour at higher elevations. Earth Planet. Sci. Lett. 307, 271-278.

Carmichael, J.D., Joughin, I., Behn, M.D., Das, S., King, M.A., Stevens, L., Lizarralde, D., 2015. Seismicity on the western Greenland Ice Sheet: Surface fracture in the vicinity of active moulins. J. Geophys. Res. Earth Surf. 120, 1082-1106.

Catania, G.A., Neumann, T.A., Price, S.F., 2008. Characterizing englacial drainage in the ablation zone of the Greenland ice sheet. J. Glaciol. 54, 567-578.

Chandler, D.M., Wadham, J.L., Lis, G.P., Cowton, T., Sole, A., Bartholomew, I., Telling, J., Nienow, P., Bagshaw, E.B., Mair, D., Vinen, S., Hubbard, A., 2013. Evolution of the subglacial drainage system beneath the Greenland Ice Sheet revealed by tracers. Nat. Geosci. 6, 195-198.

Chu, W., Creyts, T.T., Bell, R.E., 2016. Rerouting of subglacial water flow between neighboring glaciers in West Greenland. J. Geophys. Res. Earth Surf. 121, 925-938.

Cooper, M.G., Smith, L.C., Rennermalm, A.K., Miège, C., Pitcher, L.H., Ryan, J.C., Yang, K., Cooley, S., 2018. Meltwater storage in low-density near-surface bare ice in the Greenland ice sheet ablation zone. Cryosph. 12, 955-970.

Cowton, T., Nienow, P., Sole, A., Wadham, J., Lis, G., Bartholomew, I., Mair, D., Chandler, D., 2013. Evolution of drainage system morphology at a land-terminating Greenlandic outlet glacier. J. Geophys. Res. Earth Surf. 118, 29-41.

D'Odorico, P., Rigon, R., 2003. Hillslope and channel contributions to the hydrologic response. Water Resour. Res. 39, 1113.

de Fleurian, B., Morlighem, M., Seroussi, H., Rignot, E., van den Broeke, M.R., Kuipers Munneke, P., Mouginot, J., Smeets, P.C.J.P., Tedstone, A.J., 2016. A modeling study of the effect of runoff variability on the effective pressure beneath Russell Glacier, West Greenland. J. Geophys. Res. Earth Surf. 121, 1834-1848.

de Fleurian, B., Werder, M.A., Beyer, S., Brinkerhoff, D.J., Delaney, I.A.N., Dow, C.F., Downs, J., Gagliardini, O., Hoffman, M.J., Hooke, R.L., Seguinot, J., Sommers, A.N., 2018. SHMIP The subglacial hydrology model intercomparison Project. J. Glaciol., 1-20.

Fettweis, X., Franco, B., Tedesco, M., van Angelen, J.H., Lenaerts, J.T.M., van den Broeke, M.R., Gallée, H., 2013. Estimating the Greenland ice sheet surface mass balance contribution to future sea level rise using the regional atmospheric climate model MAR. Cryosph. 7, 469-489.

Flowers, G.E., 2015. Modelling water flow under glaciers and ice sheets. Proc. Math Phys. Eng. Sci. 471, 20140907.

Flowers, G.E., 2018. Hydrology and the future of the Greenland Ice Sheet. Nat. Commun. 9, 2729.

Hancock, G.R., Martinez, C., Evans, K.G., Moliere, D.R., 2006. A comparison of SRTM and high-resolution digital elevation models and their use in catchment geomorphology and hydrology: Australian examples. Earth Surf. Process. Landf. 31, 1394-1412.

Hewitt, I.J., 2013. Seasonal changes in ice sheet motion due to melt water lubrication. Earth Planet. Sci. Lett. 371-372, 16-25.

Hoffman, M., Price, S., 2014. Feedbacks between coupled subglacial hydrology and glacier dynamics. J. Geophys. Res. Earth Surf. 119, 414-436.

Hoffman, M.J., Andrews, L.C., Price, S.F., Catania, G.A., Neumann, T.A., Lüthi, M.P., Gulley, J., Ryser, C., Hawley, R.L., Morriss, B., 2016. Greenland subglacial drainage evolution regulated by weakly connected regions of the bed. Nat. Commun. 7, 13903.

Hoffman, M.J., Perego, M., Andrews, L.C., Price, S.F., Neumann, T.A., Johnson, J.V., Catania, G., Lüthi, M.P., 2018. Widespread Moulin Formation During Supraglacial Lake Drainages in Greenland. Geophys. Res. Lett. 45, 778-788.

Hubbard, B., Nienow, P., 1997. Alpine subglacial hydrology. Quat. Sci. Rev. 16, 939-955.

Karlstrom, L., Yang, K., 2016. Fluvial supraglacial landscape evolution on the Greenland Ice Sheet. Geophys. Res. Lett. 43, 2683-2692.

Karlstrom, L., Zok, A., Manga, M., 2014. Near-surface permeability in a supraglacial drainage basin on the Llewellyn Glacier, Juneau Icefield, British Columbia. Cryosph. 8, 537-546.

Koziol, C.P., Arnold, N., 2018. Modelling seasonal meltwater forcing of the velocity of land-terminating margins of the Greenland Ice Sheet. Cryosph. 12, 971-991.

Lampkin, D.J., VanderBerg, J., 2014. Supraglacial melt channel networks in the Jakobshavn Isbræ region during the 2007 melt season. Hydrolo. Process. 28, 6038-6053.

Larour, E., Seroussi, H., Morlighem, M., Rignot, E., 2012. Continental scale, high order, high spatial resolution, ice sheet modeling using the Ice Sheet System Model (ISSM). J. Geophys. Res. Earth Surf. 117.

Manning, R., 1891. On the flow of water in open channels and pipes. Trans. Inst. Civ. Eng. Irel. 20, 161-207.

McGrath, D., Colgan, W., Steffen, K., Lauffenburger, P., Balog, J., 2011. Assessing the summer water budget of a moulin basin in the Sermeq Avannarleq ablation region, Greenland ice sheet. J. Glaciol. 57, 954-964.

Meierbachtol, T., Harper, J., Humphrey, N., 2013. Basal Drainage System Response to Increasing Surface Melt on the Greenland Ice Sheet. Science 341, 777-779.

Montgomery, D.R., Foufoula-Georgiou, E., 1993. Channel network source representation using digital elevation models. Water Resour. Res. 29, 3925-3934.

Nienow, P.W., Sole, A.J., Slater, D.A., Cowton, T.R., 2017. Recent Advances in Our Understanding of the Role of Meltwater in the Greenland Ice Sheet System. Current Climate Change Reports 3, 330-344.

Noh, M.-J., Howat, I.M., 2015. Automated stereo-photogrammetric DEM generation at high latitudes: Surface Extraction with TIN-based Search-space Minimization (SETSM) validation and demonstration over glaciated regions. GIsci. Remote Sens. 52, 198-217.

Noh, M.-J., Howat, I.M., 2017. The Surface Extraction from TIN based Search-space Minimization (SETSM) algorithm. ISPRS J. Photogramm. Remote Sens. 129, 55-76.

Noh, M.-J., Howat, I.M., 2018. Automatic relative RPC image model bias compensation through hierarchical image matching for improving DEM quality. ISPRS J. Photogramm. Remote Sens. 136, 120-133.

Palmer, S., Shepherd, A., Nienow, P., Joughin, I., 2011. Seasonal speedup of the Greenland Ice Sheet linked to routing of surface water. Earth Planet. Sci. Lett. 302, 423-428.

Poinar, K., Dow, C.F., Andrews, L.C., 2019. Long-Term Support of an Active Subglacial Hydrologic System in Southeast Greenland by Firn Aquifers. Geophys. Res. Lett. 46, 4772-4781.

Schoof, C., 2010. Ice-sheet acceleration driven by melt supply variability. Nature 468, 803.

Shepherd, A., Hubbard, A., Nienow, P., King, M., McMillan, M., Joughin, I., 2009. Greenland ice sheet motion coupled with daily melting in late summer. Geophys. Res. Lett. 36.

Singh, P.K., Mishra, S.K., Jain, M.K., 2014. A review of the synthetic unit hydrograph: from the empirical UH to advanced geomorphological methods. Hydrolog. Sci. J. 59, 239-261.

Smith, L.C., Chu, V.W., Yang, K., Gleason, C.J., Pitcher, L.H., Rennermalm, A.K., Legleiter, C.J., Behar, A.E., Overstreet, B.T., Moustafa, S.E., Tedesco, M., Forster, R.R., LeWinter, A.L., Finnegan, D.C., Sheng, Y., Balog, J., 2015. Efficient meltwater drainage through supraglacial streams and rivers on the southwest Greenland ice sheet. Proc. Natl. Acad. Sci. 112, 1001-1006.

Smith, L.C., Yang, K., Pitcher, L.H., Overstreet, B.T., Chu, V.W., Rennermalm, A.K., Ryan, J., Cooper, M.G., Gleason, C.J., Tedesco, M., 2017. Direct measurements of meltwater runoff on the Greenland ice sheet surface. Proc. Natl. Acad. Sci. 114, E10622-E10631.

Snyder, F.F., 1938. Synthetic unit-graphs. Eos, Trans. Amer. Geophys. Union 19, 447-454.

Sommers, A., Rajaram, H., Morlighem, M., 2018. SHAKTI: Subglacial Hydrology and Kinetic, Transient Interactions v1.0.

Geosci. Model Dev. 11, 2955-2974.

van de Wal, R.S.W., Smeets, C.J.P.P., Boot, W., Stoffelen, M., van Kampen, R., Doyle, S.H., Wilhelms, F., van den Broeke, M.R., Reijmer, C.H., Oerlemans, J., Hubbard, A., 2015. Self-regulation of ice flow varies across the ablation area in south-west Greenland. Cryosph. 9, 603-611.

5    Werder, M.A., Hewitt, I.J., Schoof, C.G., Flowers, G.E., 2013. Modeling channelized and distributed subglacial drainage in two dimensions. J. Geophys. Res. Earth Surf. 118, 2140-2158.

Yang, K., Karlstrom, L., Smith, L.C., Li, M., 2017. Automated high resolution satellite image registration using supraglacial rivers on the Greenland Ice Sheet. IEEE J. Sel. Topics Appl. Earth Observ. Remote Sens. 10, 845-856.

Yang, K., Smith, L.C., 2016. Internally drained catchments dominate supraglacial hydrology of the southwest Greenland Ice

10    Sheet. J. Geophys. Res. Earth Surf. 121, 1891–1910.

Yang, K., Smith, L.C., As, D.v., Pitcher, L.H., Cooper, M.G., Li, M., 2019. Seasonal evolution of supraglacial lakes and rivers on the southwestern Greenland Ice Sheet. J. Geophys. Res. Earth Surf.

Yang, K., Smith, L.C., Karlstrom, L., Cooper, M.G., Tedesco, M., van As, D., Cheng, X., Chen, Z., Li, M., 2018. A new surface meltwater routing model for use on the Greenland Ice Sheet surface. Cryosph. 12, 3791-3811.

15    Zhang, W., Montgomery, D.R., 1994. Digital elevation model grid size, landscape representation, and hydrologic simulations. Water Resour. Res. 30, 1019-1028.
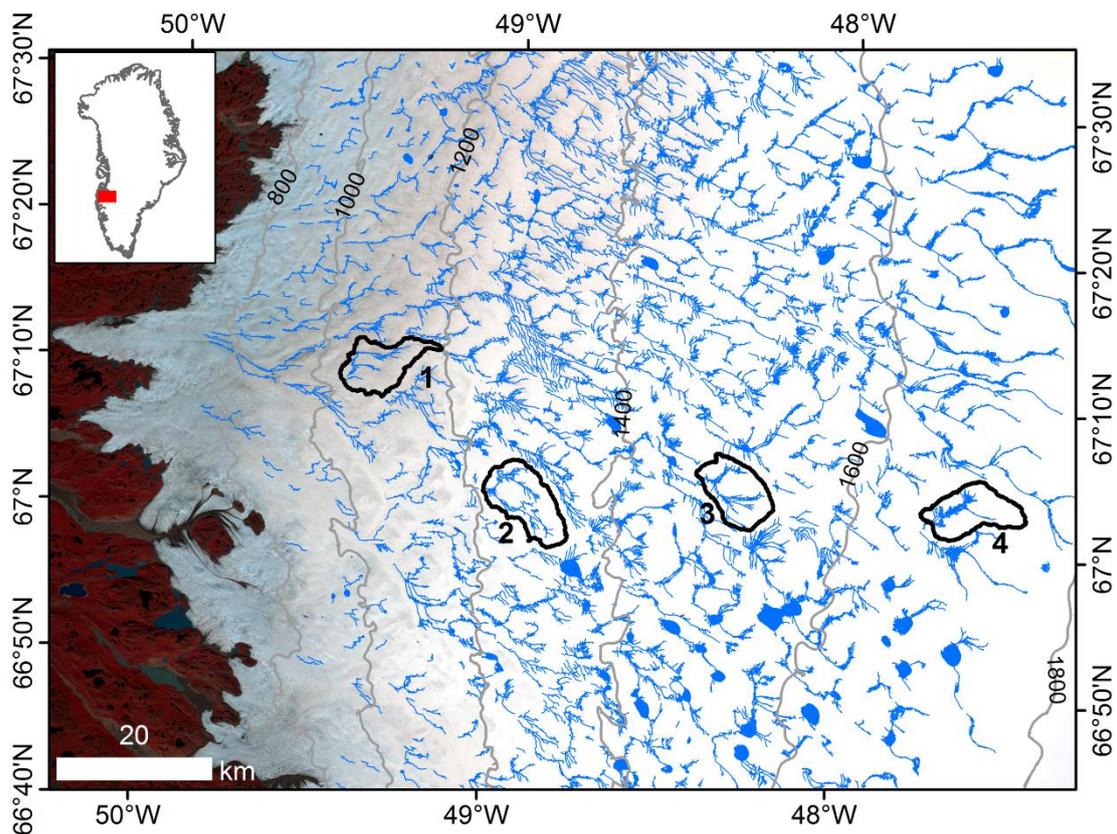
**Figure 1. Four supraglacial internally drained catchments (IDCs) on the southwest Greenland Ice Sheet were selected for inter-comparison of surface meltwater routing models. IDC topographic boundaries (black lines) are extracted from high-resolution (2 m) ArcticDEMs. Supraglacial river networks and lakes (blue lines) are mapped from a Landsat-8 panchromatic image (Yang and Smith, 2016). Base map is 10 m Sentinel-2 image acquired on 30 July 2018.**
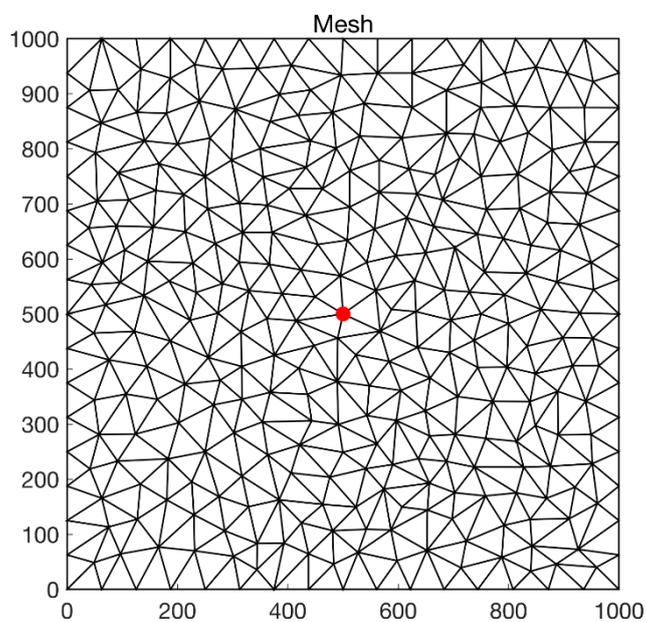
**Figure 2. The unstructured finite element mesh on a 1 km square domain used for subglacial hydrology simulations. The simulated moulin location (red dot) is located at the center of the domain and outflow is to the left.**
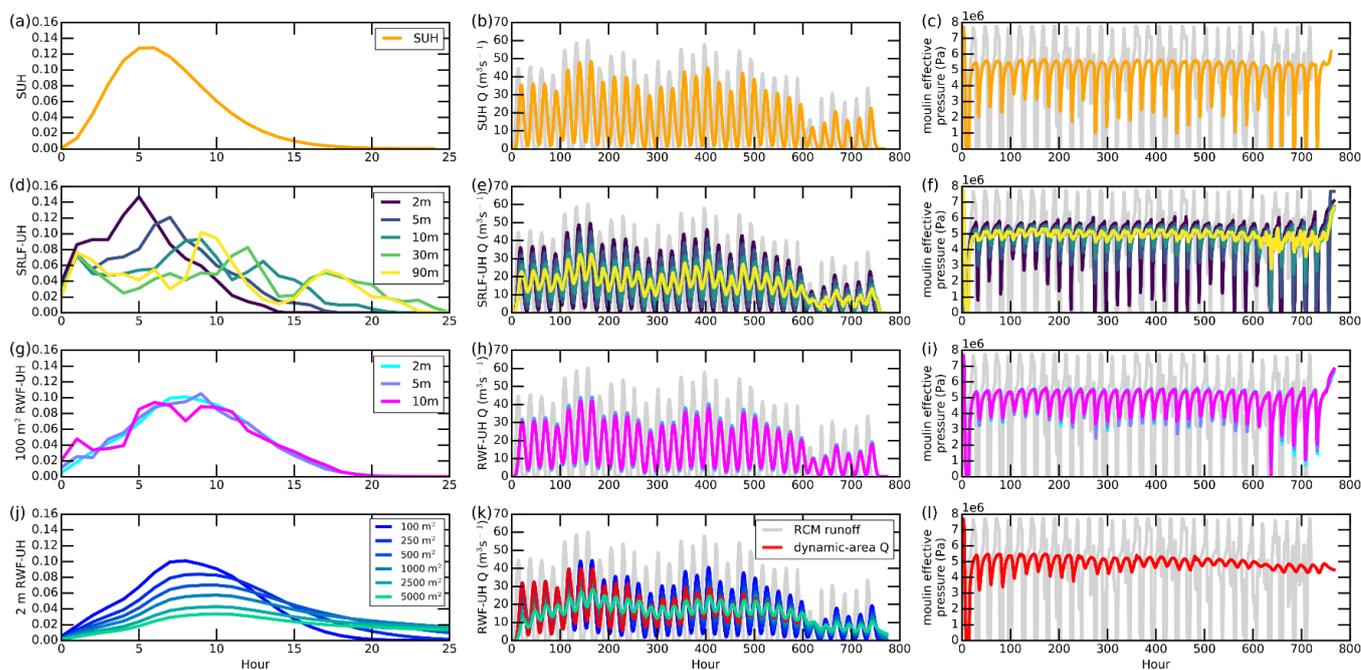
**Figure 3.** Presentation of Unit Hydrographs (UHs) (column 1), moulin discharges (column 2), and effective pressures at the moulin location on the bed (column 3) of IDC1 during July 2015, as simulated by three supraglacial routing models (SUH, RWF, and SRLF) and the SHAKTI subglacial hydrology model.
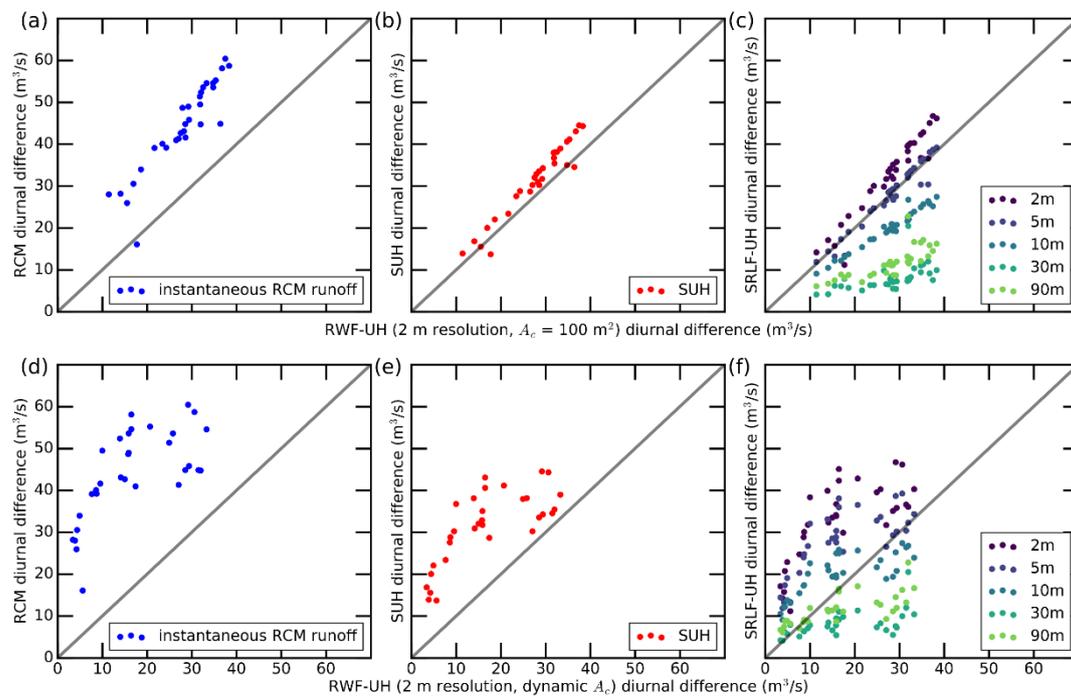
**Figure 4.** Scatter plots of RWF-routed moulin diurnal discharge range (difference between maximum and minimum moulin discharge) vs. those modeled from (a) RCM instantaneous runoff, (b) SUH routing and (c) SRLF routing. (d)-(f) are corresponding scatter plots using dynamic RWF-UHs derived from variable accumulative contributing area (Ac) to route surface meltwater.
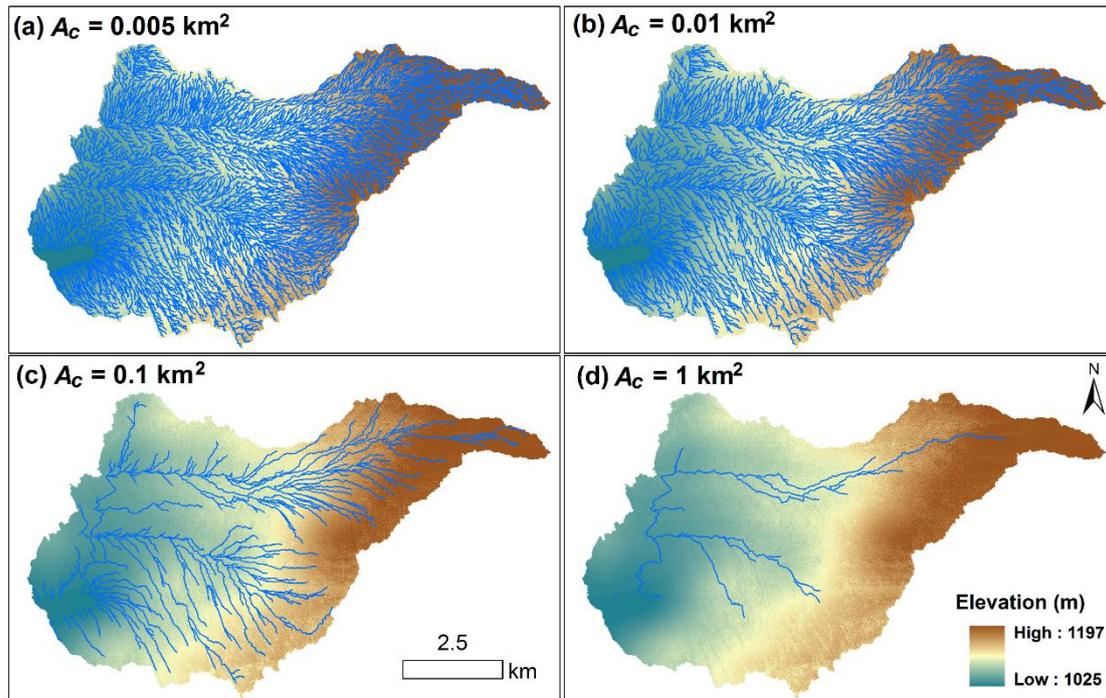
**Figure 5. Variable supraglacial stream/river network for IDC1, as simulated by applying variable accumulative area threshold ($A_c$) values to ArcticDEM. Smaller Ac yields a highly-developed supraglacial stream/river network, whereas larger $A_c$ yields a poorly-developed one. Varying Ac can thus be used to mimic the seasonal evolution of supraglacial stream/river networks.**
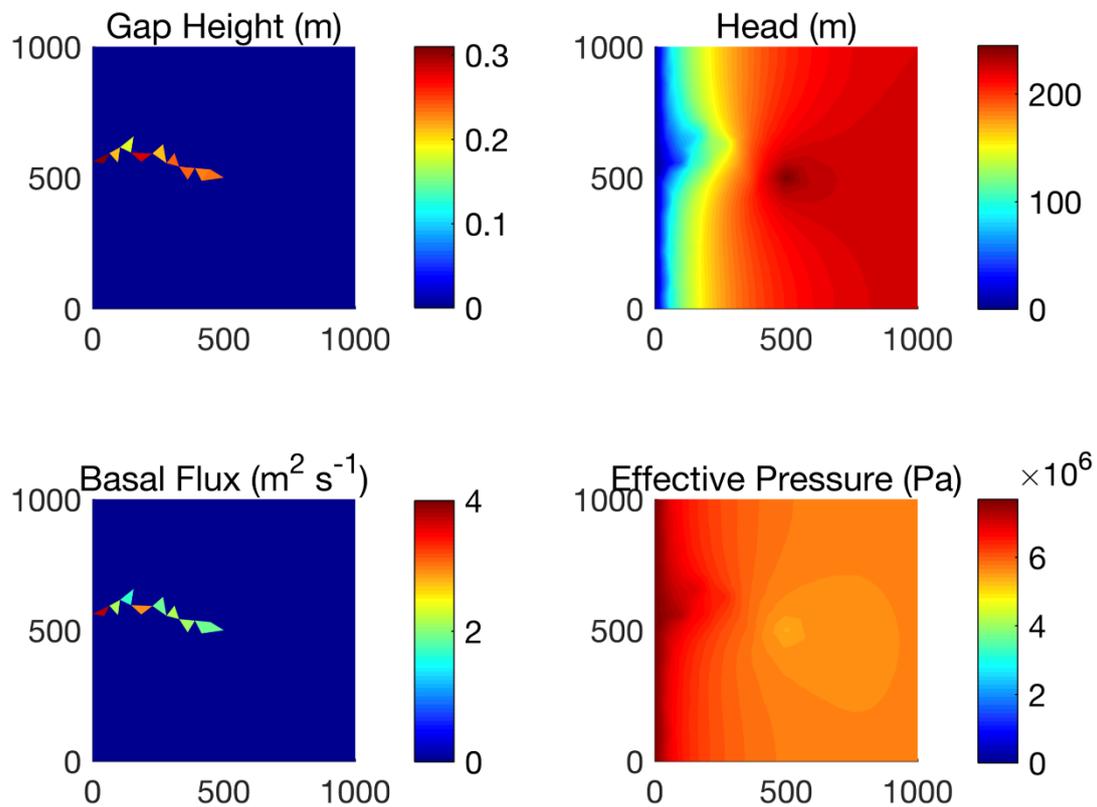
**Figure 6. Snapshots of subglacial hydrology fields on day 23 in IDC1 using the SUH routing method to drive moulin input (see full animation of channel evolution and fluctuation in the Supplemental Animation). An efficient channelized drainage pathway develops from the moulin location at the center of the domain to the outflow at the left, characterized by higher gap height, water flux, effective pressure, and lower hydraulic head than its surroundings in the y direction.**
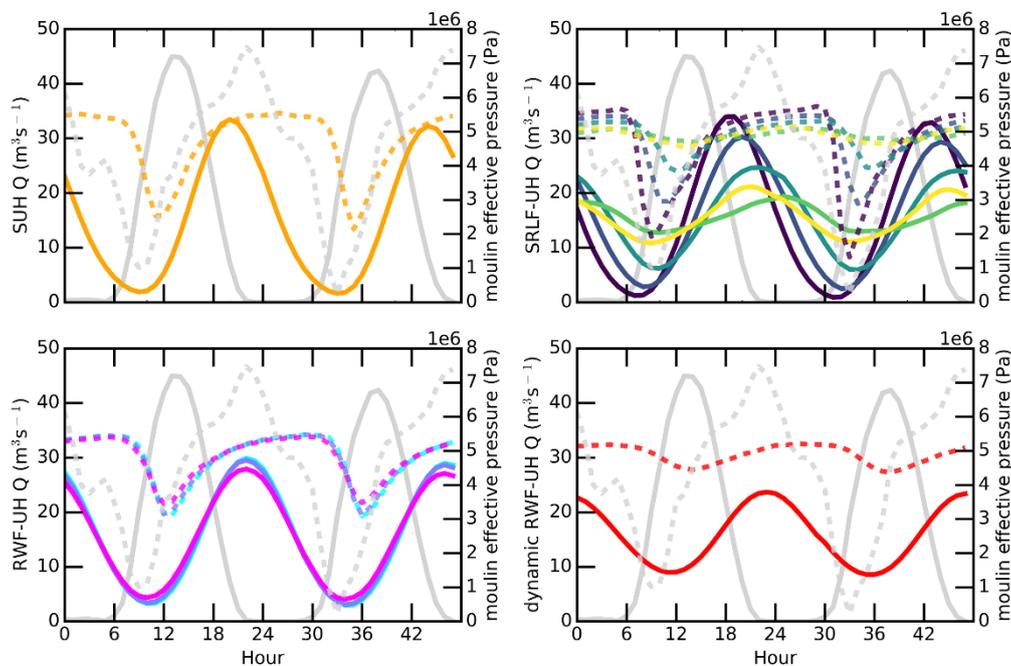
**Figure 7. The average two-day cycle of moulin discharge (*Q*) for IDC1 during July 2015 derived from Figure 3. The daily minimum input in supraglacial moulin discharge (solid lines) is followed within 12 hours by the daily minimum effective pressure (dashed lines). This suggests that the system becomes highly pressurized with low input as the subglacial gap shuts down due to creep, then opens up due to melt as discharge increases again. As the new water inputs are accommodated, efficient pathways reform and effective pressure increases (effective pressure decreases).**

**Table 1. Summary of four study catchments.**

| Catchment ID | | IDC1 | IDC2 | IDC3 | IDC4 |
|---|---|---|---|---|---|
| Area (km²) | | 53.0 | 66.9 | 57.3 | 58.5 |
| Mean Elevation (m) | | 1086 | 1282 | 1510 | 1672 |
| Ice thickness (m) | | 854 | 936 | 1259 | 1432 |
| Distance to ice edge (km) | | 25 | 40 | 70 | 100 |
| Peak discharge time | RCM | 13-15 | 13-15 | 13-14 | 13-14 |
| | SUH | 19-20 | 20-21 | 19-20 | 19-20 |
| | SRLF 2m, 5m, 10m, 30m, 90m | 18-19, 20-21, 21-22, 22-23, 22-23 | 18-19, 19-20, 21-22, 21-22, 21-22 | 17-18, 18-19, 20-21, 22-23, 22-23 | 17-18, 19-20, 23, 23, 23 |
| | RWF | 22-23 | 21-22 | 20-21 | 21-22 |

**Table 2. Constants and parameters used in subglacial hydrology simulations.**

| Symbol | Value | Units | Description |
|--------|-------|-------|-------------|
| $\rho_w$ | 1000 | kg m$^{-3}$ | Bulk density of water |
| $\rho_i$ | 910 | kg m$^{-3}$ | Bulk density of ice |
| A | $5\times10^{-25}$ | Pa$^{-3}$ s$^{-1}$ | Ice flow-law parameter |
| n | 3 | Dimensionless | Ice flow-law exponent |
| $b_r$ | 0.1 | m | Typical height of bed bumps |
| $l_r$ | 2.0 | m | Typical spacing between bed bumps |
| $u_b$ | $10^{-6}$ | m s$^{-1}$ | Sliding velocity (31.5 m a$^{-1}$) |
| g | 9.8 | m s$^{-2}$ | Gravitational acceleration |
| $\omega$ | 0.001 | Dimensionless | Parameter controlling nonlinear transition between laminar and turbulent flow |
| L | $3.34 \times 10^5$ | J kg$^{-1}$ | Latent heat of fusion of water |
| G | 0.05 | W m$^{-2}$ | Geothermal flux |
| $c_t$ | $7.5 \times 10^{-8}$ | K Pa$^{-1}$ | Change of pressure melting point with temperature |
| $c_w$ | $4.22 \times 10^3$ | J kg$^{-1}$ K$^{-1}$ | Heat capacity of water |
| $\upsilon$ | $1.787 \times 10^{-6}$ | m$^2$ s$^{-1}$ | Kinematic viscosity of water |
| $e_v$ | 0 | Dimensionless | Englacial void ratio |